BENCHMARKING A LIGHT-CURVE MODEL AT LOW-Z

FREDERICK J. MAYER[1] and JOHN R. REITZ[2]

[1]*Mayer Applied Research Inc., 1417 Dicken Drive, Ann Arbor, MI;*
E-mail: fmayer@sysmatrix.net
[2]*2260 Chaucer Court, Ann Arbor, MI*

(Received 11 August 2004; accepted 3 September 2004)

Abstract. A set of well-measured, low-z, type Ia supernovae from the Calán/Tololo SNe data sets is used to determine benchmark parameters in our hydrodynamics-based, light-curve model. The light-curve data fit fairly well in B, V, and R passbands but not as well in the I passband. The fitting procedure, extracted best-fit model parameters, and their connection to type Ia SN parameters are presented. Our benchmarked light-curve model represents an alternative to empirical template methods for the analysis of light-curve data.

Keywords: type Ia supernovae, light-curves

1. Introduction

Using type Ia supernovae (hereinafter SNe Ia) as "standard candles" for cosmological distance indicators would be both accurate and simple were it not for the slight magnitude differences within this class of SNe (Branch and Tamman, 1992). Phillips (1993) has shown that a correlation exists between the peak magnitude and the fall rate after peak luminosity of the SNe Ia such that the peak magnitude is slightly smaller for the faster declining SNe. A number of template and parameterization procedures have been developed to take account of this variation in order to obtain a corrected value of the peak magnitude. It is, of course, crucial to do so when the SNe magnitudes are being used for cosmological measurements where small errors in magnitude could translate to large errors in distance. The reader is referred to the article by Leibundgut (2001, and references therein) for an excellent review of the light-curve parameterization procedures and uncertainties when using the SNe Ia as standard candles in cosmology. As an alternative to the light-curve parameterization methods, we have developed a theoretical light-curve model that is constrained by the conservation laws of hydrodynamics to allow direct comparison between the magnitude observations and the assumed parameters of the SN. One purpose of the present paper is to benchmark the light-curve model by fitting it to some well-measured SNe Ia data sets and to extract certain parameters for future use. The Calán/Tololo data sets (29 light-curves) are chosen for this purpose. A second purpose is to examine the systematic differences between the model calculations and the observations.

The model has allowed us to quantify the observed slight magnitude variations (those that exhibit the decreasing peak magnitude with increasing decline rate)

Astrophysics and Space Science **294:** 241–253, 2004.

and to understand the various controlling parameters of the SNe Ia, especially the nearby SNe Ia. If the characterization low-z data are well-fit by the model, then extension to higher-z can be considered.

Our light-curve model, hereinafter referred to as MRb, has been described previously (Mayer and Reitz, 2002). A summary of the model is presented in Section 2. In Section 3, we compare MRb with light-curve data from the Calán/Tololo SNe data sets (C/TSNe) described by Hamuy et al. (1996a, 1996b), obtain our "best-fits" to a selected sample of C/TSNe and examine systematic effects in these data/model comparisons. In Section 4, we discuss connections between some model parameters. In Section 5, we provide fits to all (except two) the C/TSNe data sets and in Section 6 we discuss some energy constraints.

We point out that our light-curve model is not a detailed simulation of the type Ia supernova explosion and evolution such as has been carried out by, for example, Pinto and Eastman (2000) and Höflich, Müller, and Khoklov (1993). Such simulations are very important in understanding the spectra and detailed structure of the light curves. Our model, on the other hand, is a relatively simple picture of the explosion/hydrodynamics which allows us to quantify magnitude variations and light-curve shape from some basic parameters of the explosion. Because it conserves mass, momentum, and energy in a unified model description, the model shows how the luminosity and other features of the light-curve depend upon certain combinations of input SN/progenitor parameters. Furthermore, it shows how energy availability (from nuclear fuel and possibly gravity) may limit the luminosity. But because it predicts how the light-curve shape is affected by the fractional conversion of the nuclear material to Ni-Co-Fe, the model can be used as an alternative to the template method for the characterization of SNe Ia light curves at low-z and high-z.

As with many physics models, our light curve model has limitations. However, the limitations in simple models, when compared to data, often suggest refinements in the physics and sometimes even new directions for experiments. We hope this is the case with our MRb model.

2. The MRb Light-Curve Model

Our MRb model (Mayer and Reitz, 2002) is derived from a self-similar approximation to the spherically symmetric hydrodynamic equations conserving mass, momentum, and energy. It models the large-scale dynamics with a Gaussian density profile, a linear velocity profile and a time-dependent scale-height $y(t)$. The scale-height determines the time evolution of the SN expansion. Because it conserves mass, momentum, and energy in a unified model description, MRb relates the properties at later stages of expansion to the basic parameters of the progenitor and the explosion. These parameters are the mass m measured in units of the solar mass, the initial radial mass scale r in units of the solar radius, the energy release E_{sn}

(we use the parameter $\nu = E_{sn}/E_g$ where E_g is the gravitational potential energy of the progenitor just before explosion), and ϵ which measures the fractional conversion of the star's mass to ^{56}Ni. The density at the center is $\rho_0 = 80.6m/r^3$, and the characteristic time is $\tau = 354[r^3/m]^{1/2}$. The temperature at the center (in eV) [from Eqs. (10) of MRb] is given by $\theta_c = 18\,670\,m^{1/2}/r$. We have taken $m = 1.4$ in all cases presented below. The normalized radial density scale $y(t)$ is calculated from the ordinary differential equation [Eq. (7) of MRb], given by

$$y\ddot{y} + \dot{y}^2/2 = (1/\tau^2)[\nu f(t) - (1 - 1/y)] \tag{1}$$

where $f(t)$ is the explosion energy function: $f(t) = 1 - \exp(-t/t_1) + f_{rad}$ and where f_{rad} (proportional to ϵ) contains the Ni-Co-Fe decay chain [see MRb]. With a numerical integration of Eq. (3) above, the total luminosity is calculated assuming thermal radiation (see Appendix) from a surface located at $R_s = 0.236\eta r y(t) R_\odot$ and is given by

$$L_{sn}/L_\odot = 1.7 \times 10^{15}(m/r)^2\eta^2 \exp(-\eta^2)[\tau^2 y\ddot{y} + (4/\sqrt{2}y)]/y \tag{2}$$

with η fixed at $\eta = 2.0$. Finally, a bolometric correction is applied and the results are converted to absolute magnitudes.

As discussed in the Appendix, the observed radiation spectra are clearly not Planckian. This would appear to severely compromise our model. However, we find that the temperature we calculate from the model yields a Planck function fit to an observed spectrum that, on average, fits fairly well.

3. Benchmark Parameters

Using C/TSNe (Hamuy et al., 1996a,b), we have established the benchmark model parameters by selecting the four SNe having magnitude data prior to peak light; they are SN1992bc, SN1992bo, SN1992al, and SN1993O. The first three have been observed in the B, V, R, and I passbands, the last in B, V, and I. Distance moduli were calculated from the data in Hamuy et al. (1996a) and taking a Hubble constant $H_0 = 72$ km/(s Mpc). We have done least squares fits to the data sets varying the parameters in the MRb model differential equation (see Appendix). As we had found previously, the data sets could be well-fit with just one value, each, of r (the initial scale size), and ν (the SN explosion energy in units of its gravitational potential energy) and m (the mass of the SN). Only the single parameter ϵ (the fractional mass conversion to ^{56}Ni) had to be adjusted to fit the different SNe Ia data sets. In Section 4, we discuss the relationships among some of these parameters. Many more data sets having points before the peak will need to be examined to provide more confidence in the value $\nu = 1.30$ found using the selected four SNe.

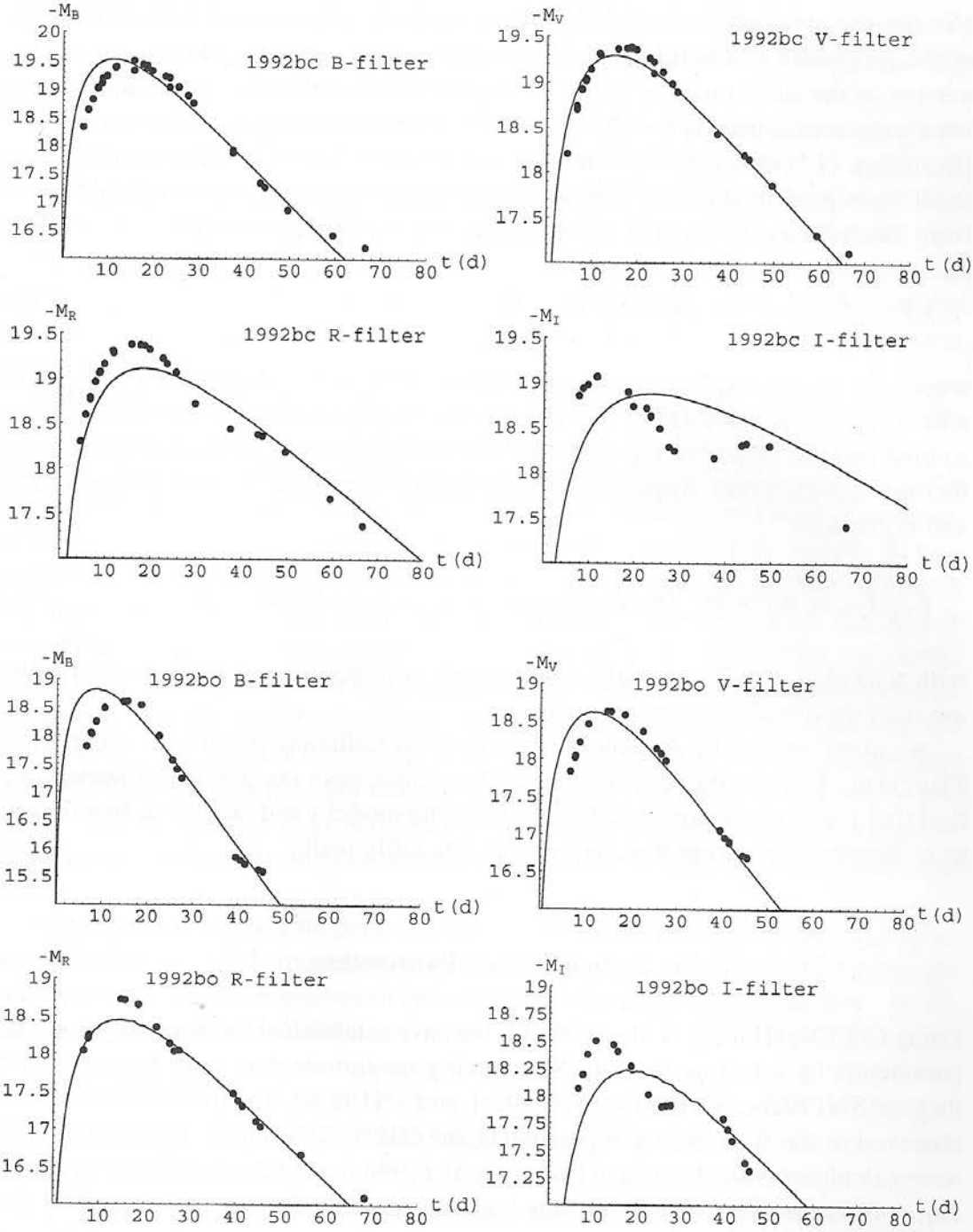

Figure 1. The absolute magnitude data (points) and model integration (solid lines) for SN1992bc and SN1992bo in the V, B, R, and I filterbands.

Figures 1 and 2 show the best-fits between the MRb model and the four selected SNe data sets. The procedure was to iteratively adjust, the time zero offset of the data and the various parameters until a minimum least squares error was achieved in the B, V, R, and I filterbands. As is clear from the Figures, the I filterband data are

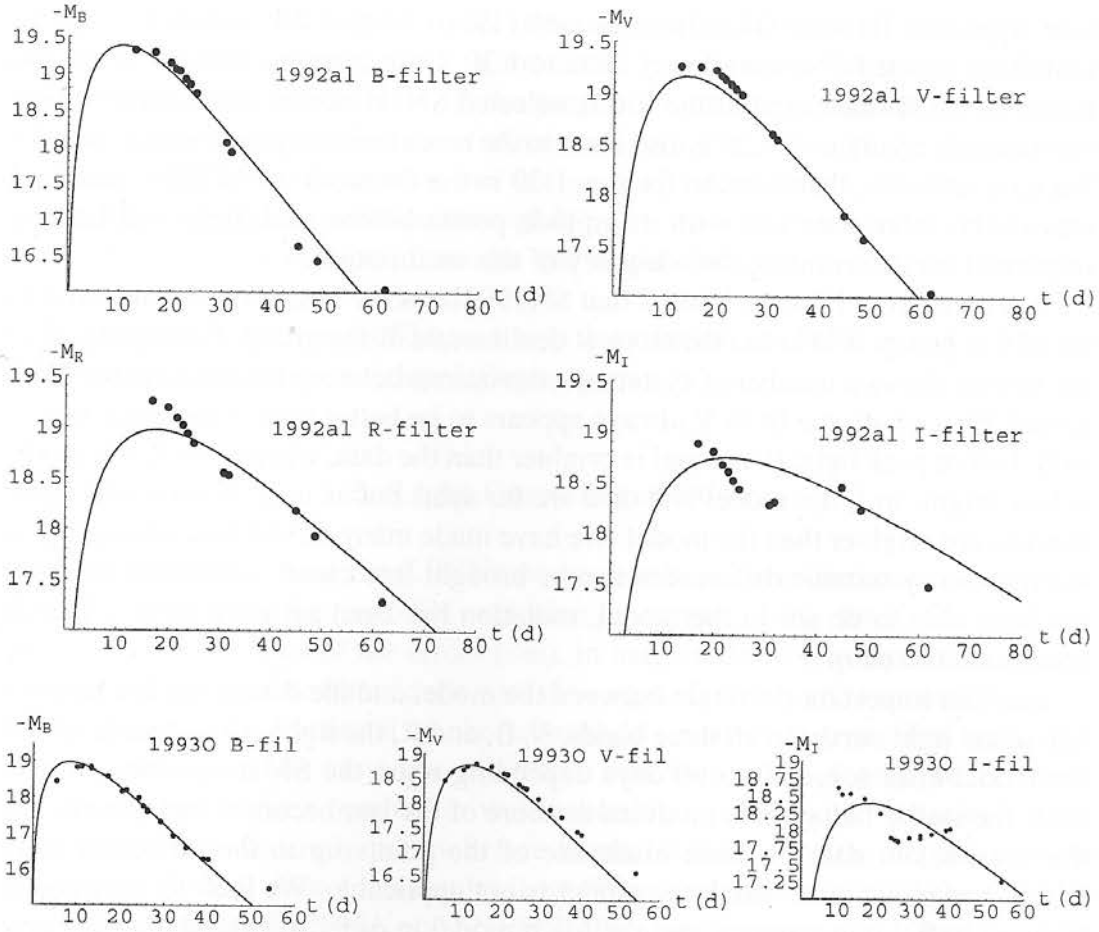

Figure 2. The absolute magnitude data (points) and model integration (solid lines) for SN1992al in the V, B, R, and I filterbands and SN1993O in the B, V, and I passbands.

systematically anomalous but was still included in the least squares minimization. Except for the I filterband, the fits to the data are fairly good, but they are not perfect. Table I displays the best-fit set of benchmark parameters for the selected SNe. For these SNe, only a small correction from $z = 0$ is expected. However, we did make the appropriate small z-dependent K-corrections to our MRb model. The bandpass filter functions used in the bolometric correction (BC) calculations

TABLE I

MRb model parameters

SN	m	ν	ϵ	r
1992bc	1.4	1.30	0.34	0.0038
1992bo	1.4	1.27	0.15	0.0038
1992al	1.4	1.32	0.29	0.0038
1993O	1.4	1.29	0.17	0.0038

(see Appendix B) were taken from Bessell (1990). Notice that values of ν for the first three selected SNe are all very close to 1.30. Unfortunately, there were no data points in the R filter band of the fourth selected SN. However, that minimization, even though giving $\nu = 1.29$ is also close to the model minimization with $\nu = 1.30$. We have choosen, therefore, to fix $\nu = 1.30$ in the fits to all the C/TSNe data sets. Obviously, more data sets with magnitude points before peak light will be very important for determining the adequacy of this assumption.

It is clear from Figures 1 and 2 that SN1992bc is the best and most useful data set of this group. It also has the slowest decline rate of the group. Examining all of the figures shows a number of systematic deviations between the data and the MRb model. First of all, the fit in V always appears to be better than in the other bands. In B, before peak light, the model is brighter than the data, whereas in R, the model is less bright. In I, the model and data are far apart but as in R, before peak light, the data are brighter than the model. We have made many model runs attempting to see if these systematic differences can be brought into closer agreement but have not been able to do so. In the model, radiation has been assumed to be a Planck spectrum at fixed η.

Another important deviation between the model and the data is the discrepancy late in the light curve. In all three bands, V, B, and R, the light-curve data lie above the model after some 50 to 60 days depending upon the SN in question. In late time, the stellar radiation is modified as more of the star becomes transparent. For this reason, our data fits have made use of the points up to the inflection point in the data plots, after which the model is not applicable. We look to incorporate changes in SN transparency into the MRb model in order to extend it to higher-z SNe. Furthermore, we expect that as more low-z SNe Ia data sets become available, it should be possible to better understand the origins of the deviations between the observations and the MRb model.

We note again that observations (Phillips, 1993) of a correlation between the peak magnitude of the light-curve and the faster decline rate in B are clearly seen to be reproduced in our model curve fits; they result from different fractional conversion of the progenitor's mass to the iron group elements. We note that there are other correlations between the decline rates in the other bands as can be seen from the figures.

4. Progenitor Density and Temperature Relationship

When we started this work, we had hoped to extract more useful progenitor parameters directly from the fitting of the light-curve data and the model. However, although the fits are fairly good, the density and central temperature at ignition in the model cannot be uniquely determined. It is possible to show, using Eqs. (1, 2), that the luminosity (with ϵ held constant) scales as

$$L_{\rm sn} \propto mr/(\nu - 1). \tag{3}$$

So, for the same mass progenitor, any combination of r, ν with the same value of $r/(\nu - 1)$ gives identical fits to the data. The combination listed in Table I results in a central temperature of the progenitor, at ignition, of about 6 MeV, a value consistent with estimates of Arnett (1969). Even though the progenitor's central density and temperature are not uniquely determined, the data do constrain them to be a combination through Eq. (3). It should be noted that the value $\nu = 1.30$ which we obtained from the fits would change if we changed the value of r.

Taking $\nu = 1.30$, $r = 0.0038$, and $m = 1.4$ converts the MRb model of Section 2 to a one parameter system depending only on ϵ.

5. Light-Curve Data Fitting

The light-curve data from the C/TSNe study were fit using an iterative procedure as follows. Guessing at the $t = 0$ SN explosion point, and a value for ϵ, we calculated the sum of the squares of the errors (sse), in magnitudes, between the model and the data in the available filter bands with $\Delta = a_B \text{sseB} + a_V \text{sseV} + a_R \text{sseR} + a_I \text{sseI}$ where the as are the fractional number of total data points in a given filter band. The sum was minimized by varying ϵ and then a new starting $t = 0$ point was chosen. Iterating in this fashion resulted in well-behaved minimum in all cases examined with the proviso that only points before about 60 days after the explosion were employed. Table II shows the results from fitting our MRb model to the C/TSNe data base except for SN1992K and SN1992J. The data points for these latter two SNe were too late to be used with the model. In Table II, we display the sum of the squares of the errors in each filter band (sseB, sseV, sseR, and sseI), the root-mean square error (rmse in magnitudes) is given by rmse = $(\text{sseB} + \text{sseV} + \text{sseR} + \text{sseI})^{1/2}$, the number of data points used in the minimization (ndpt), and finally, the root mean square error per data point.

There are substantial differences in the quality of the model fits in the C/TSNe data sets as can be seen in Table II. However, the average rms errors per data point are generally not very large, less than 0.04 magnitudes. And the actual data sets for all these cases fit the light curves predicted by the model fairly well. Figure 3 displays the model-data fits for five additional SNe form C/TSNe data sets. We note here again that the only parameter having been adjusted for these fits was the value of ϵ. From the best-fit data shown in Table II, we find the frequency of occurence at different values of ϵ in these low-z SNe. There were 10 having $0.14 \leq \epsilon \leq 0.19$, 9 having $0.20 \leq \epsilon \leq 0.25$, 4 having $0.26 \leq \epsilon \leq 0.30$, and 4 having $0.30 \leq \epsilon \leq 0.34$. We have examined the data in Table II for possible correlations with z, for example, but haven't found any.

A single data set fit represents many thousands of iterative numerical integrations of the model differential equations – a formidable task for large scale hydrodynamic simulations.

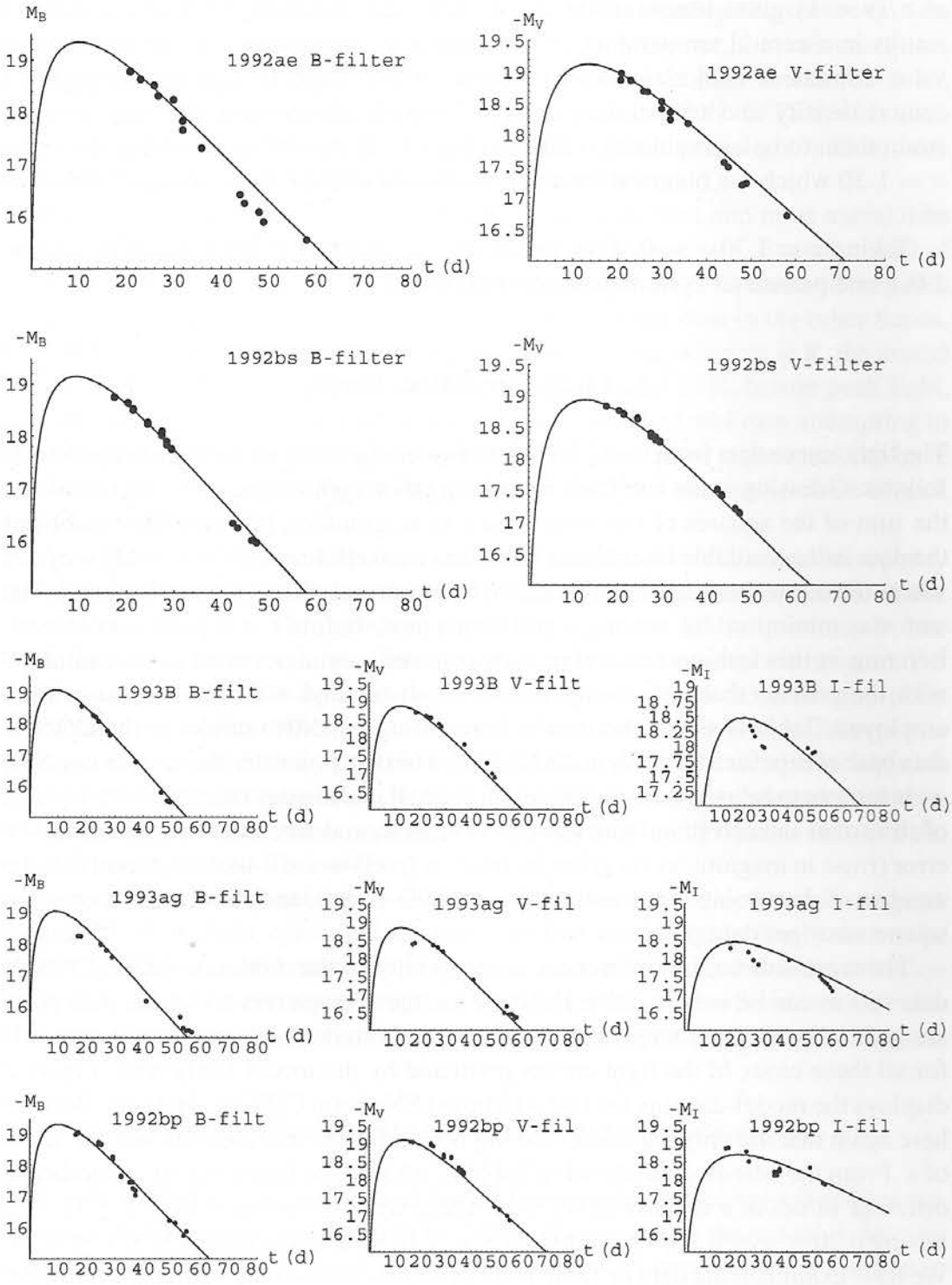

Figure 3. The absolute magnitude data (points) and model integration (solid lines) for SN1992ae and SN1992bs in the V and B filter bands; also SN1993B, 1993ag, and 1992bp in the V, B, and I filter bands.

TABLE II

Data fitting results ($m = 1.4$, $\nu = 1.30$ for all cases)

SN	z	ϵ	sseB	sseV	sseR	sseI	rmse	ndpt	rmse/ndpt
1990af	0.0506	0.16	0.831	0.394	–	–	1.11	47	0.024
1990O	0.0303	0.28	0.128	0.122	0.067	0.328	0.803	20	0.040
1990T	0.0404	0.22	0.251	0.107	0.092	0.483	0.889	27	0.033
1990Y	0.0391	0.33	0.214	0.113	0.0468	0.116	0.721	26	0.028
1991ag	0.0141	0.34	0.343	0.199	0.0469	0.073	0.813	43	0.019
1991S	0.0546	0.28	1.24	0.119	0.099	0.096	1.25	54	0.023
1991U	0.0317	0.33	0.35	0.180	0.129	0.264	0.960	48	0.02
1992ae	0.0752	0.26	1.09	0.213	–	–	1.14	29	0.039
1992ag	0.0249	0.22	0.361	0.391	–	0.011	0.874	22	0.04
1992al	0.0146	0.29	0.563	0.162	0.274	0.675	1.29	50	0.026
1992aq	0.1018	0.17	0.669	0.204	–	1.07	1.39	37	0.038
1992au	0.0614	0.23	0.286	0.123	–	1.11	1.23	18	0.069
1992bc	0.0202	0.34	2.58	0.405	1.44	4.17	2.93	108	0.027
1992bg	0.0352	0.2	0.144	0.107	–	0.482	0.856	32	0.027
1992bh	0.0452	0.22	0.123	0.129	–	0.326	0.760	36	0.021
1992bk	0.0481	0.18	0.668	0.115	–	1.15	1.39	27	0.052
1992bl	0.0437	0.18	0.765	0.279	–	0.344	1.18	33	0.036
1992bo	0.0189	0.15	2.82	1.07	0.340	1.29	2.35	70	0.034
1992bp	0.0793	0.25	0.549	0.375	–	0.703	1.28	55	0.023
1992br	0.0882	0.14	1.07	0.170	–	–	1.11	19	0.059
1992bs	0.0637	0.21	0.114	0.0502	–	–	0.405	33	0.012
1992P	0.0252	0.23	0.194	0.0344	–	0.453	0.825	19	0.043
1993ag	0.049	0.19	0.902	0.388	–	0.866	1.47	38	0.039
1993ah	0.0297	0.20	0.166	0.090	–	0.140	0.629	13	0.048
1993B	0.0707	0.19	0.077	0.214	–	0.493	0.885	29	0.030
1993H	0.0239	0.15	0.498	0.238	0.162	0.162	1.03	50	0.021
1993O	0.051	0.17	1.05	0.707	–	1.38	1.77	60	0.030
Ave	0.0456	0.226	0.669	0.248	0.270	0.705	1.16	39	0.0333

6. Energy Considerations in the MRb Model

The increasing gravitational energy of the unstable contracting white dwarf (WD) produces high temperatures which ignite C-O and subsequent nuclear reactions which produce the explosion in the SN. If we compare the energies of the system just before the original WD begins contraction and at a late stage of the explosion, we can write

$$(\nu - 1)E_{\mathrm{g}} + E'_{\mathrm{g}} + E_{\mathrm{loss}} = E_{\mathrm{nuc}} \tag{4}$$

where E_g is the gravitational potential energy of the collapsed WD just before the explosion and E'_g is the gravitational energy of the WD before collapse. We have added an E_{loss} term (for radiation and neutrino emission) since our hydrodynamic model does not include them in the energy balance equation. E_{nuc} is the energy produced in the nuclear reactions which convert C–O to iron-group elements.

As noted, the explosive energy in our model is given by νE_g that is proportional to $\nu\rho_0^{1/3}$. But $(\nu - 1)\rho_0^{1/3}$ is the only combination of ρ_0 and ν (see Section 4) that we can determine from fitting the theory to the data (ρ_0 is the central density of the collapsed WD). We cannot determine ρ_0 absolutely, but since it is related to the central temperature and this temperature must be high enough for the nuclear reactions to proceed at a sufficiently rapid rate, ρ_0 must be larger than $3 \times 10^7 \text{g/cm}^3$. We expect, however, the central density to be very much higher. Nonetheless, the first term in Eq. (2) is proportional to $(\nu - 1)\,\rho_0^{1/2}$ which is determined by our model.

It is convenient to divide all energies in Eq. (2) by the mass of the star, so that each term represents an energy per unit mass. In SN1992bc, we have $\nu = 1.30$, $r = 0.0038$, $\rho_0 = 2 \times 10^9$ g/cm^3. This yields $(\nu - 1)E_g = 3.5 \times 10^{17}$ ergs/g. With an initial central density of 4×10^5 g/cm^3 in the original (uncollapsed) WD, its $E'_g = 10^{17}$ ergs/g. E_{loss} may be the same order of magnitude as E'_g. Assuming that there is no neutron star remnant left by the SN, the sum of these energies must equal $E_{nuc} \approx 7 \times 10^{17}$ ergs/g. This energy, available from the nuclear conversion of C–O material to ^{56}Ni (which powers the SN light-curve), appears to be adequate. There is, of course, the possibility that a neutron-star remnant is left behind, and its gravitational energy could provide an addition source of energy for the explosion.

7. Discussion

We have characterized the MRb model with four well-measured SNe at low-z. Other C/TSNe data sets have been examined for testing the single parameter (ϵ) fitting procedure. On all of the data sets examined, the procedure has worked quite well. Our model, constrained by the conservation laws of hydrodynamics, represents an alternative to empirical (and statistical) algorithms for determining absolute magnitudes. To extend our model to higher-z, a method for calculating of the K-corrections, sensitive to the spectral shapes, must be determined. Also, the effects of late-time transparency of the radiating plasma has to be understood.

Although we have used a curve-fitting procedure to constrain the model parameters, we note that these parameters are physical quantities connected to the progenitor and the explosion, yet they manifest themselves in the characteristics of the light-curve. In addition, we find that a single parameter, ϵ (the fraction of the progenitor mass burned to ^{56}Ni) accurately accounts for the variation in light output and decline rate in the data sets that we have examined, although there are clearly systematic deviations from the model light-curves. More low-z data sets

having sufficient data before and after peak light should help to unravel the origin of these deviations.

Acknowledgements

The authors thank David Branch and Mario Hamuy for helpful suggestions.

Appendix

A. The Planck Spectrum Approximation

It has been firmly established [see Hamuy et al. (2002) and Branch et al. (2003), and references therein] that the spectra from Type Ia SNe are far from a Planck spectrum. So, this has raised the question as to why our Planck assumption works as well as it does in reproducing the light-curve shapes displayed above. The answer is that the fitting procedure determines a "best-fit" temperature as a function of time averaged over all the various filter bands.

In Figure 4, we display a spectrum from 1999ee at peak-light in B, obtained by Hamuy et al. (2002) along with a "best-fit" Planck spectrum with temperature $\theta = 0.71$ eV. The Planck spectrum clearly fits poorly in many wavelength regions but "on-average" it fits reasonably well. Our MRb model fits the light-curve data

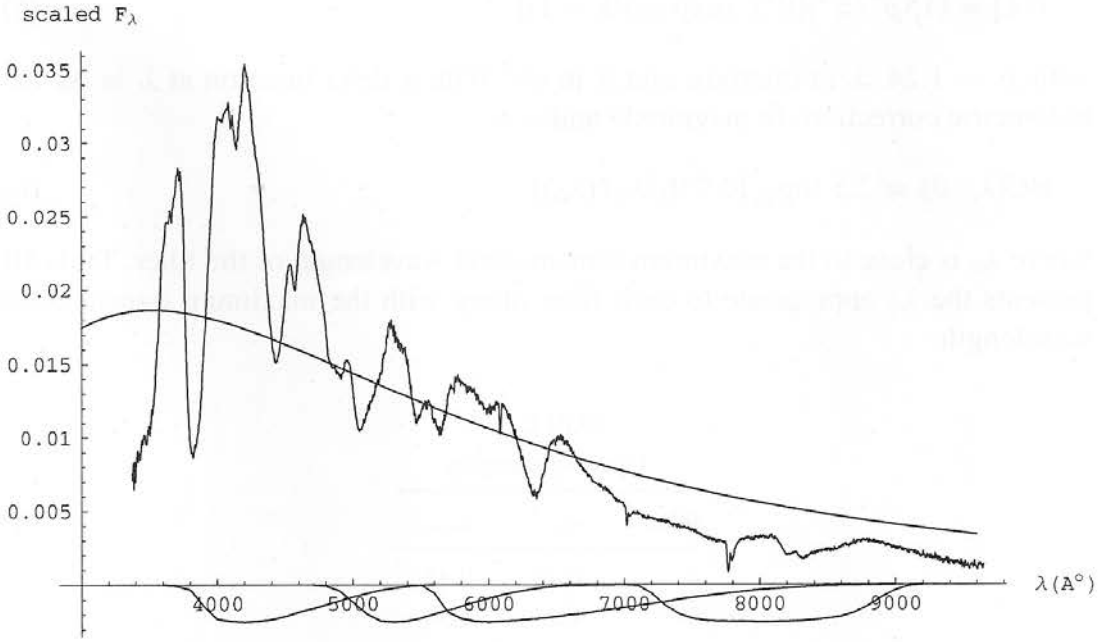

Figure 4. The optical spectrum of 1999ee at peak-light in B and the "best-fit" Planck curve having $\theta = 0.71$ eV. The filterbands B, V, R, and I, are arrayed at the bottom of the figure.

from the SN, at peak light in B, with a temperature, $\theta = 0.77$ eV. This value is obtained from the best-fit model for all of the data points in all filterbands. Notice that at before peak light in B, the model temperature appears to be somewhat higher than the Planck-fit temperature. Still, we conclude that the Planck radiation assumption is quite useful as a first approximation for the light-curve data fittings. The model generally overestimates the B data points before peak light in B, generally fits the V data points fairly well, and generally underestimates the R and I data points. Some of these differences are likely attributible to the inaccuracy of the Planck radiation approximation by noting how the wavelength bands span across the actual spectra and the Planck-fit in Figure 4. But some other phenomena are likely contributing to the differences in the R and I bands.

As mentioned previously, large hydrodynamic-radiation calculations like those of Pinto and Eastman (2000) and Höflich, Müller, and Khoklov (1993) will be required to obtain detailed information about the SN radiation and explosion.

B. Bolometric and K corrections

We have calculated the bolometric corrections by integrating the product of a Planck spectrum and the filter passband over wavelength for each filter. The filter bandpass functions were those of Bessell (1990). The numerical integrations were compared to a delta-function approximation (see Narlikar, 1983) and were found to be quite accurate and easier to use in data fitting. Following Narlikar, the normalized spectral intensity function, here a Planck distribution, is given by

$$I(\lambda) = (15p^4/\pi^4)[\theta^4\lambda^5(\exp p/\theta\lambda - 1)]^{-1} \tag{5}$$

with $p = 1.24$, λ in microns, and θ in eV. With a delta function at $\lambda = \lambda_0$ the bolometric correction (in magnitude units) is

$$\mathrm{BC}(\lambda_0, \theta) = 2.5 \log_{10} [0.736/\lambda_0 I(\lambda_0)] \tag{6}$$

where λ_0 is close to the maximum transmission wavelength of the filter. Table III presents the λ_0 appropriate to each filter along with the maximum transmission wavelength.

TABLE III

Filter wavelengths

Filter	λ_0	λ_{max}
B	0.42	0.42
V	0.53	0.53
R	0.63	0.60
I	0.77	0.80

The $K(z, \lambda_0)$ corrections are similarly found to be

$$K(z, \lambda_0) = 2.5 \log_{10}(1 + z) - 2.5 \log_{10}[I(\lambda_0/(1 + z)]/I(\lambda_0)] \quad (7)$$

using the value of λ_0 appropriate to each filter.

References

Arnett, W.D.: 1969, *Astrophys. Space Sci.* **5**, 180–212.
Bessell, M.S.: 1990, *Pub. A.S.P.* **102**, 1181.
Branch, D. and Tamman, G.A.: 1992, *Annu. Rev. Astron. Astrophys.* **30**, 359–389.
Branch, D., et al.: 2003, *Astron. J.* **126**, 1489–1498.
Hamuy, M., et al.: 1996, *Astron. J.* **112**, 2398, paper a.
Hamuy, M., et al.: 1996, *Astron. J.* **112**, 2408, paper b.
Hamuy, M., et al.: 2002, *Astron. J.* **124**, 417–429.
Höflich, P., Müller, E. and Khoklov, A.: 1993, *Astron. Astrophys.* **268**, 570–590.
Leibundgut, B.: 2001, *Annu. Rev. Astrophys.* **39**, 67.
Mayer, F.J. and Reitz, J.R.: 2002, *Astrophys. Space Sci.* **282**, 439–445.
Narlikar, J.V.: 1983, *Introduction to Cosmology*, Jones and Bartlett Publishers, Inc, Boston, p. 359.
Phillips, M.M.: 1993, *Astrophys. J.* **413**, L105–108.
Pinto, P.A. and Eastman, R.G.: 2000, *Astrophys. J.* **530**, 744–777.